

## MCS Monte Carlo Simulation of APR1400 Benchmark

Fathurrahman Setiawan, Deokjung Lee\*

Department of Nuclear Engineering, Ulsan National Institute of Science and Technology, 50 UNIST-gil, Ulsan, 44919, Republic of Korea

\*Corresponding author: [deokjung@unist.ac.kr](mailto:deokjung@unist.ac.kr)

### 1. Introduction

The high-fidelity neutron transport simulation using Monte Carlo (MC) method for whole core calculation is becoming more frequently performed due to its advantage on producing more accurate results relative to deterministic method. MCS [1] is a MC code developed at Ulsan National Institute of Science and Technology (UNIST) since 2011, had been used to solve many whole core problems ranging from criticality problems to multi-physics simulation. APR1400 benchmark is a product of cooperation program between United States and Republic of Korea called US/ROK I-NERI which has purpose on improving high-fidelity multi-physics simulation code for advanced nuclear reactors [2]. The benchmark provides detailed description of geometry and material composition which refer to the submitted APR1400 Design Control Document. There are six categories of problem provided: 1) 2D fuel pin, 2) 2D fuel assembly, 3) 2D core, 4) 3D core, 5) Control rod worth and 6) 3D core depletion. Except the last category, benchmark results from McCARD Monte Carlo simulation developed in KAERI are provided. In this article, those results are compared against MCS in similar manner in terms of nuclear data and modelling parameter. An addition on multi-physics depletion result from MCS is also presented.

### 2. Benchmark Description

The APR1400 reactor has a 17-by-17 core lattice with total of 241 assemblies. Each assembly consists of 236 pin cells and 5 tube cells that occupy 2-by-2 pin cell size. The assembly lattice is a rectangular with size of 16-by-16 and pitch of 20.7772 cm. There are 9 types of fuel assemblies, distinguished by the enrichment and arrangement. There are 9 spacer grids smeared to the corresponding location with its respected length. Detailed information on geometry (radial and axial) and material composition can be found explicitly described inside the documentation [2].

From the five categories of problem that has reference calculation results, there are total of 151 problems distributed as follows:

- 1) 2D fuel pin: 45 problems (5 enrichments, 3 temperatures, 3 boron concentrations)
- 2) 2D fuel assembly: 81 problems (9 FA types, 3 temperatures, 3 boron concentrations)
- 3) 2D core: 9 problems (3 temperatures, 3 boron concentrations)
- 4) 3D core: 9 problems (3 temperatures, 3 boron concentrations)

- 5) CR worth: 7 problems (7 CR insertions)

The first four of the categories consists of combination of 3 different temperatures and boron concentrations which can be categorized into operating conditions as in Table I. The operating condition for the CR worth problems is based on HZP1 where 7 different arrangements of inserted rod bank groups are simulated.

Table I: Operating conditions for APR1400 benchmark

ID number	ID name	Temperature [K]			Boron [ppm]
		Fuel	Clad	Mod	
1	CZP0	300	300	300	0
2	HZP0	600	600	600	
3	HFP0	900	600	600	
4	CZP1	300	300	300	1000
5	HZP1	600	600	600	
6	HFP1	900	600	600	
7	CZP2	300	300	300	2000
8	HZP2	600	600	600	
9	HFP2	900	600	600	

\*CZP = Cold Zero Power, HZP = Hot Zero Power, HFP = Hot Full Power

All the reference benchmark calculation with McCARD is utilizing the ENDF/B-VII.1 library where the particle histories are as follow:

- Pin problem: 200,000 histories; 50 inactive cycles; 500 active cycles
- Assembly problem: 200,000 histories; 200 inactive cycles; 500 active cycles
- Core problem: 500,000 histories; 500 inactive cycles; 500 active cycles

### 3. Calculation and Results

All the simulation with MCS is using the same ENDF/B-VII.1 library and particle histories as the benchmark calculation. The default physics options in MCS are turned on namely, free-gas thermal scattering kernel, Probability Table for unresolved resonance and Windowed-Multipole Doppler Broadening in case there is no exact ACE file for the corresponding material temperature. The thermal  $S(\alpha, \beta)$  data from ENDF/B-VII.1 version is also used for hydrogen in the moderator.

The comparison results are reported mainly in terms of reactivity difference ( $\Delta\rho$ ) and Root-Mean-Square error for the pin/assembly power comparison which can be mathematically expressed as follows:

$$\Delta\rho = \frac{1}{k_{eff}^{MCCARD}} - \frac{1}{k_{eff}^{MCS}}, \text{ [pcm]} \quad (1)$$

$$RMS = \sqrt{\frac{\sum_{i=1}^n (\epsilon)_i^2}{n}} \quad (2)$$

where,

$$\epsilon = \frac{Power_{MCS}}{Power_{McCARD}} - 1, [\%] \quad (3)$$

The statistical uncertainty of multiplication factor for MCS simulation is 8 pcm maximum while the relative error for tally results is below 1%. The convergence of simulation is ensured by evaluating the Shannon entropy and multiplication factor during the inactive cycles.

### 3.1. 2D fuel pin problems

Together with 9 combinations of the operating conditions, five different enrichments namely 1.7%, 2%, 2.64%, 3.14% and 3.64% are incorporated to generate total of 45 problems to be simulated. The multiplication factor of MCS underestimates the benchmark solution for all 45 problems as shown in Fig. 1. The maximum  $\Delta\rho$  is within the CZP operating conditions for different boron concentrations. Also, as the boron concentration increased, the difference becomes much more observable.

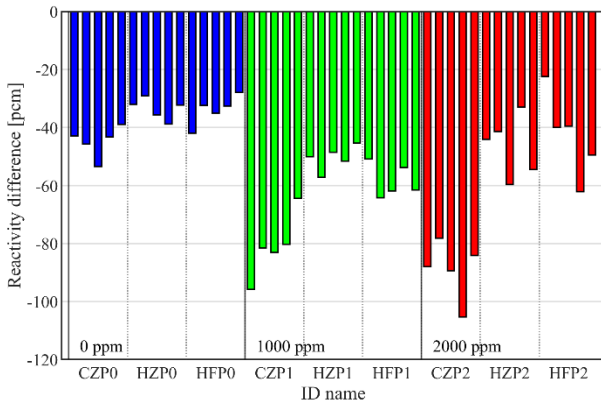


Fig. 1. Reactivity difference for fuel pin problems

### 3.2. 2D fuel assembly problems

The 2D assembly problems category consists of 81 problems where the reactivity difference and RMS error for pin power comparison are presented in Fig. 2 and Fig. 3 respectively. The  $\Delta\rho$  values behave similarly as in previous section where the CZP problem give the maximum difference against benchmark up to  $\sim 111$  pcm. For the RMS error, it shows that the assembly with burnable absorber pins give larger values, yet the maximum is  $\sim 0.27\%$ . All the pin power comparison for each problem is within the total statistical uncertainty ( $\sigma_{tot} = \sqrt{\sigma_{MCS}^2 + \sigma_{McCARD}^2}$ ) except for the burnable poison which underestimates the benchmark solution for maximum about 1%. The burnable absorber is modelled with 10 rings in MCS with intent to capture the spatial variation more accurately. However, model with only 1 ring give similar results as the 10 rings model.

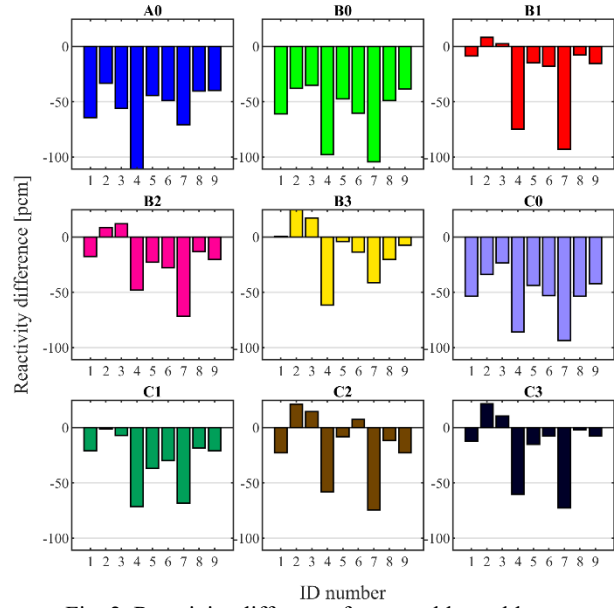


Fig. 2. Reactivity difference for assembly problems

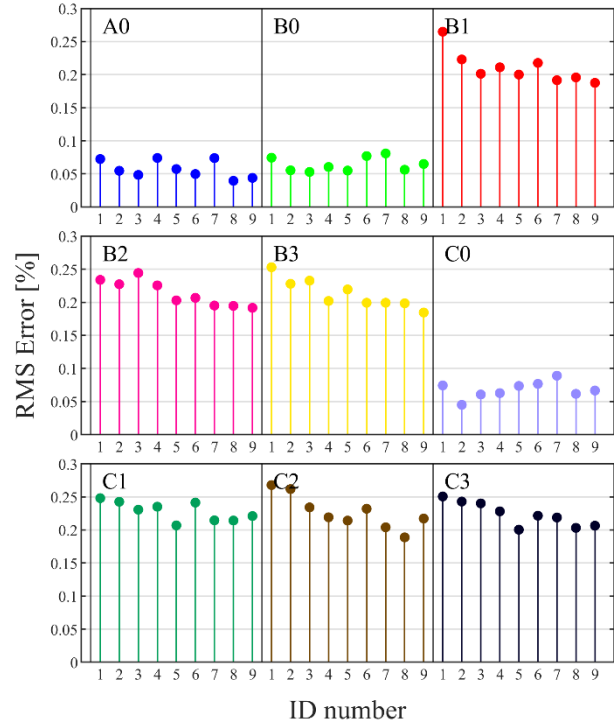


Fig. 3. RMS error for assembly problems

### 3.3. 2D core problems

The comparison result for 2D core problems is shown in Fig. 4. On the left side, the maximum reactivity difference is observed for problem CZP2 following by CZP1 and CZP0. The RMS error for the assembly power comparison reach the maximum value of 1.1% as shown on the right side of the figure. The assembly-wise power comparison for all the problems is shown in Fig. 5. The maximum assembly power difference is observed in HZP0 problem with 2.5%. The total statistical uncertainty reaches 1.5% ( $1\sigma$ ) for problem CZP2 for

assembly at the center of the core. Relatively high statistical uncertainties are observed for assembly facing the reflector or boundary condition.

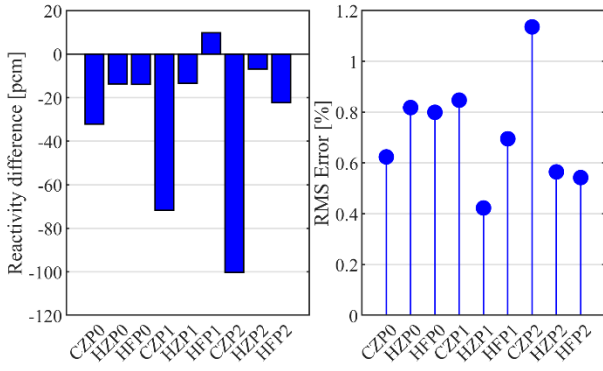


Fig. 4. Reactivity difference and RMS error for 2D core problems

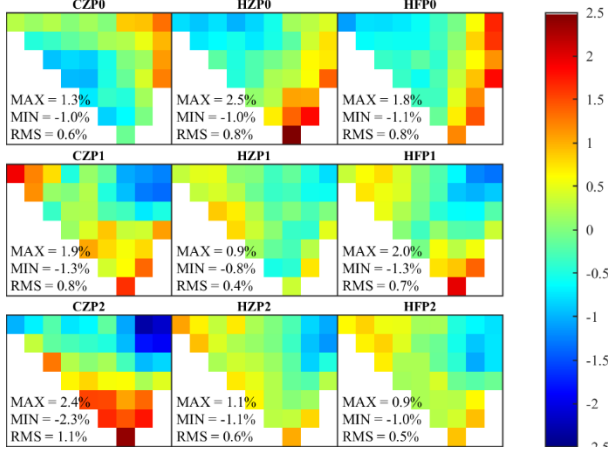


Fig. 5. Assembly power comparison for 2D core problems

### 3.4. 3D core problems

The reactivity difference and RMS error for assembly power comparison are shown in Fig. 6. Maximum multiplication factor difference is observed for problem CZP2 as well with value  $\sim 92$  pcm while the maximum RMS error is  $\sim 1.3\%$  on problem CZP1.

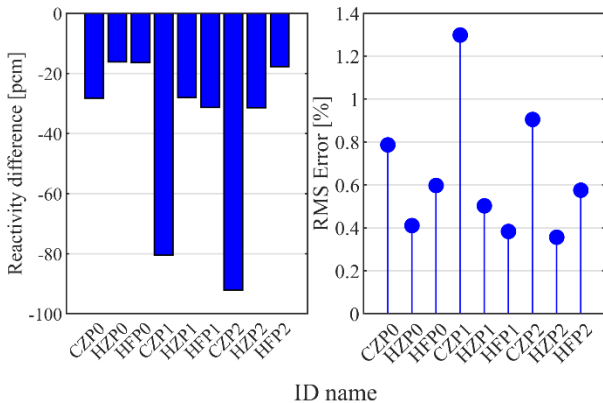


Fig. 6. Reactivity difference and RMS error for 3D core problems

Assembly-wise power comparison is presented in Fig. 7 where it shows that the MCS simulation for problem with CZP conditions (especially CZP1) underestimates the benchmark at the region near the center. Table II shows the RMS error for the difference on axial power profile between MCS and benchmark. The difference of axial power profile for all problems are shown in Fig. 8. No consistent pattern on the difference (e.g., shifted to upper or lower part of the core) which reflects the statistical traits of the simulation.

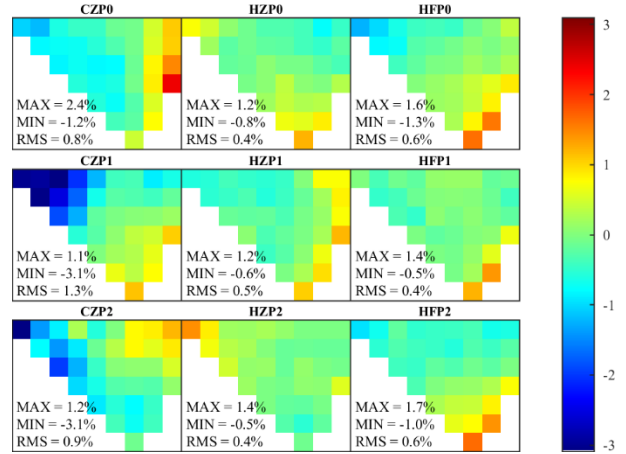


Fig. 7. Assembly power comparison for 3D core problems

Table II: RMS error of axial power for 3D core problems

ID name	RMS [%]	ID name	RMS [%]	ID name	RMS [%]
CZP0	1.24	CZP1	2.28	CZP2	1.26
HZP0	2.29	HZP1	1.87	HZP2	0.22
HFP0	1.71	HFP1	0.69	HFP2	0.48

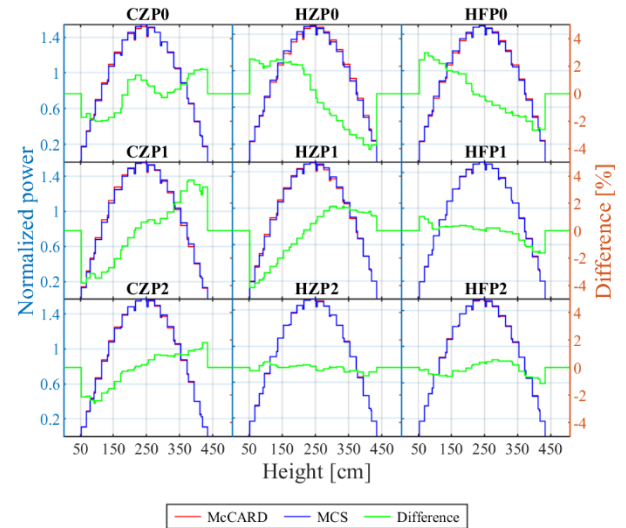


Fig. 8. Axial power profile for 3D core problems

### 3.5. Control rod worth problems

There are total of 7 CR group banks labelled as 5, 4, 3, 2, 1, B and A. The configurations for the seven rod worth problems including simulation result are listed in

Table III. The all rods out (ARO) model based on the 3D HZP0 problem. Very small differences of rod worth are observed for all problems with maximum of 14 pcm. The assembly power and axial power comparison are shown in Fig. 9 and Fig. 10 with largest RMS error of 1.5% and 2.1% respectively.

Table III: Comparison of rod worth for various bank insertion

Inserted bank(s)	MCS rod worth [pcm]	Rod worth difference [pcm]
ARO	-	-
5	366.0	-0.6
5,4	695.9	-6.0
5,4,3	1698.9	7.8
5,4,3,2	2741.4	-1.5
5,4,3,2,1	4757.6	-14.5
5,4,3,2,1,B	8906.4	11.7
5,4,3,2,1,B,A	16135.4	-14.3

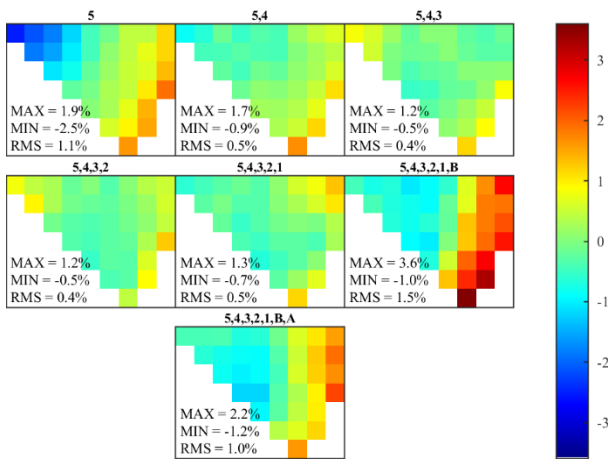


Fig. 9. Assembly power for CR worth problems

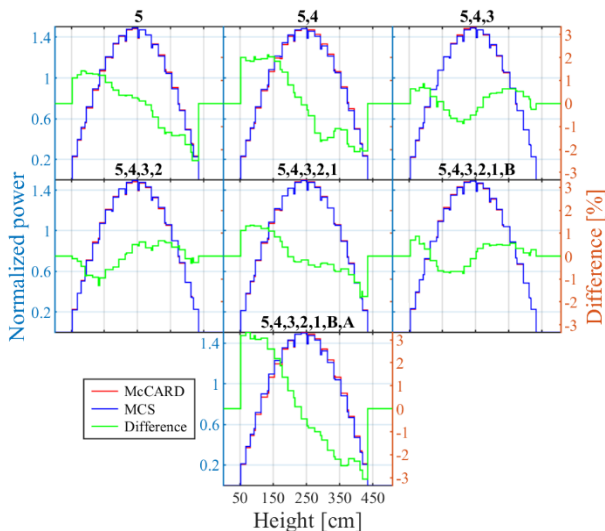


Fig. 10. Axial power profile for CR worth problems

### 3.6. Depletion problem

The single cycle depletion problem in hot full power condition is simulated with MCS utilizing the embedded

TH1D solver for thermal-hydraulics feedback. Critical boron concentrations are calculated for 21 burnup step and compared against various MOC transport codes available in references [3], [4], [5]. The result from ST3D code which also developed in our laboratory is the closest one with maximum difference of 45 ppm at the later stage of the cycle as shown in Fig. 11. NTracer result also is getting closer to MCS result after hitting the middle of cycle (MOC) while DeCART consistently differ for about 69 ppm in average. This may be because DeCART use its own thermal-hydraulics module which is different than others.

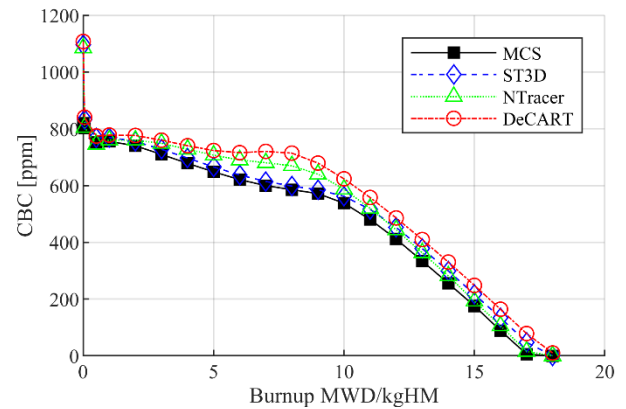


Fig. 11. CBC letdown curve from different codes

Fig. 12 shows the axial power profile during the beginning of cycle (BOC), middle of cycle (MOC) and end of cycle (EOC) which is typical for PWRs. The pin-wise radial distributions for 4 kinds of parameters are shown in Fig. 14. At the BOC, quite distinctive value relative to the neighborhoods are observed at the burnable absorber pin location.

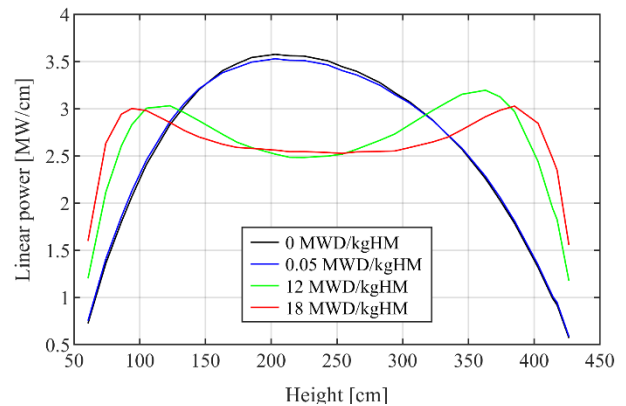


Fig. 12. Axial power profile at different stages of burnup

## 4. Supplementary Results

Persistent difference between MCS and McCARD in the CZP operating condition may occur whether because different nuclear data (especially the  $S(\alpha, \beta)$  scattering data for thermal reactor), user input definitions during the modelling, or even the physics inside the codes. Thus, to make sure that MCS physics algorithms work properly,

identical models that use exactly same nuclear data are developed using the well-known MCNP6 code [6]. Simple 2D pin problems are chosen and the comparison of multiplication factor against MCS is shown in Fig. 13.. The reactivity difference is no more than 23 pcm which likely comes from statistical uncertainty. In addition, MCS is not always underestimating MCNP6 results like when comparing against the benchmark. Thus, the result demonstrates the physics in MCS is working properly and emphasizes that there may be slightly different in the model and nuclear data used in MCS and benchmark simulation.

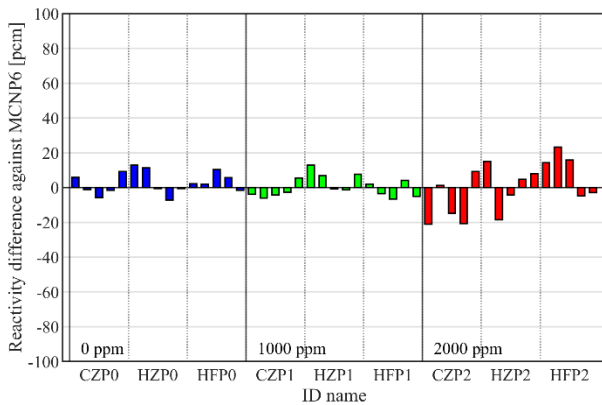


Fig. 13. Reactivity difference between MCS and MCNP6 for pin problems

## 5. Conclusion

The interpretation of APR1400 MCS benchmark problems had been done by MCS for 6 set of problem categories. MCS underestimates benchmark simulation for the first 4 categories (2D fuel pin, 2D assembly, 2D core and 3D core problems) specifically for CZP operating conditions. The differences are strongly suspected comes from the model interpretation or nuclear data specifically the thermal  $S(\alpha, \beta)$  data which backed by the supplementary comparison of MCS and MCNP6 code for identical pin problems. The result of

depletion simulation with thermal-hydraulics feedback is presented to exhibit the capability of MCS code.

## Acknowledgement

This work was supported by the National Research Foundation of Korea (NRF) grant funded by the Korea government (MSIT). (No. NRF-2019M2D2A1A03058371).

## REFERENCES

- [1] H. Lee, W. Kim, P. Zhang, A. Khassenov, Y. Jo, J. Park, J. Yu, M. Lemaire and D. Lee, "MCS - A Monte Carlo particle transport code for large-scale power reactor analysis," *Annals of Nuclear Energy*, vol. 139, 2020.
- [2] S. Yuk, "APR1400 Reactor Core Benchmark Problem Book," Technical Report RPL-INERI-CA-004, KAERI, Daejeon, South Korea, 2019.
- [3] R. Lee, "Verification of STREAM3D for APR1400 Reactor Core Benchmark," Master Thesis, Ulsan National Institute of Science and Technology, Ulsan, South Korea, 2022.
- [4] H. Hong and H. G. Joo, "Analysis of the APR1400 PWR Initial Core with the nTRACER Direct Whole Core Calculation Code and the McCARD Monte Carlo Code," in *Transactions of the Korean Nuclear Society Spring Meeting*, Jeju, South Korea, 2017.
- [5] S. Yuk and J. Y. Cho, "DeCART Solutions of APR1400 Reactor Core Benchmark Problems," in *Transactions of the Korean Nuclear Society Virtual Autumn Meeting*, South Korea, 2021.
- [6] D. B. Pelowitz, J. T. Goorley, M. R. James, T. E. Booth, F. B. Brown, J. S. Bull, L. J. Cox, J. W. D. Jr., J. S. Elson, M. L. Fensin, R. A. F. III, J. S. Hendricks, H. G. H. III, R. C. Johns, B. C. Kiedrowski, R. L. Martz, S. G. Mashnik, G. W. McKinney, R. E. Prael, J. E. Sweezy, L. S. Waters, T. A. Wilcox and A. J. Zukaitis, "MCNP6 User's Manual," Los Alamos National Laboratory, Los Alamos, NM, USA, 2013.

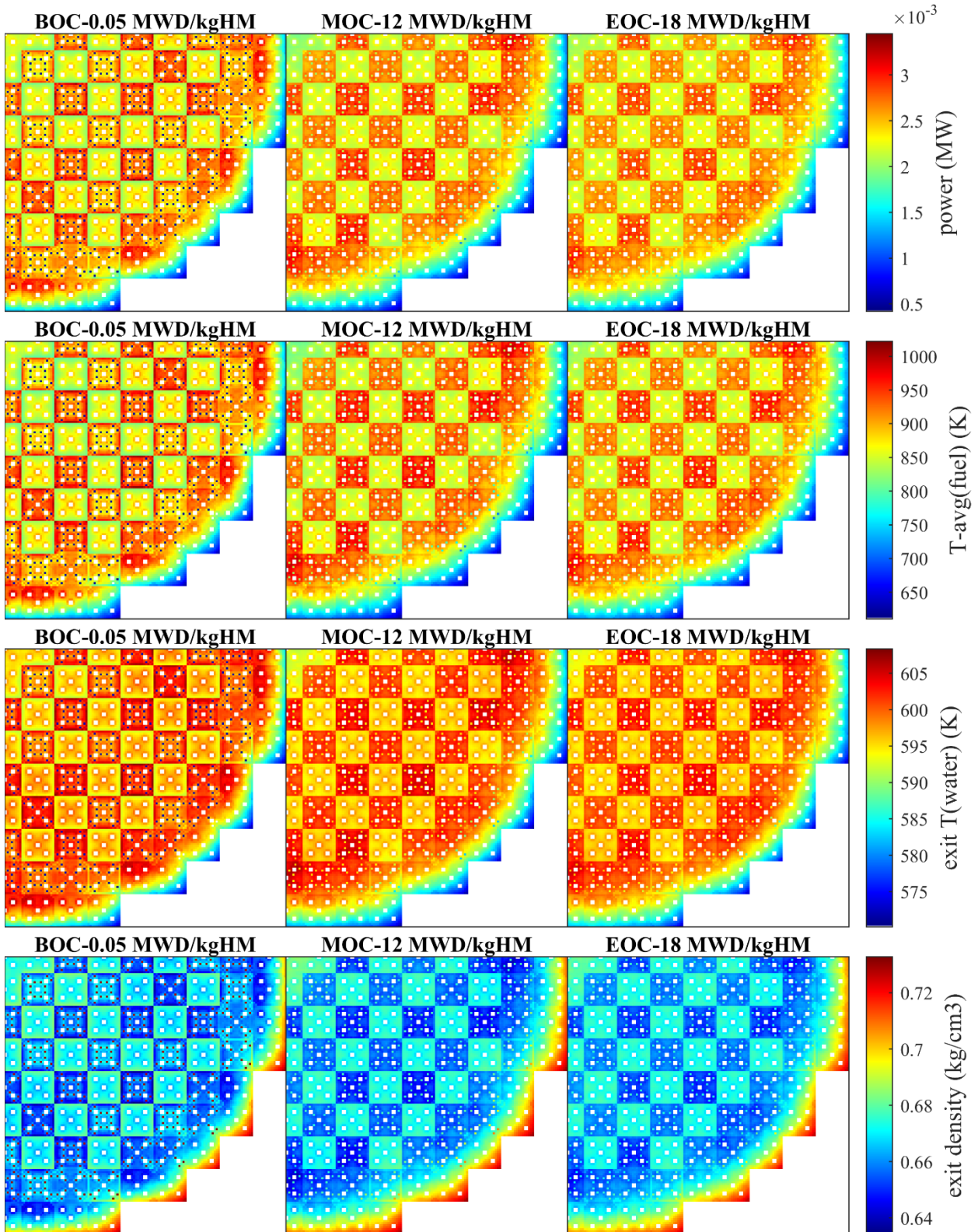


Fig. 14. Radial pin-wise distributions at different stages of burnup